Proximal Photocleavage: Controlling Polymer Solubility Through Pathway Dependent Wavelength-Orthogonal Photoreactions

*Nigel D Kidder-Wolff and Samuel W Thomas III**

N. D. Kidder-Wolff, S. W. Thomas III
Tufts University
62 Talbot St., Medford MA, 02155, USA
E-mail: sam.thomas@tufts.edu

Keywords: photocleavage, photochromes, crosslinking, decrosslinking, coumarin

Abstract

Current families of reversible photochemical reactions present challenges for light-controlled polymers of either photostationary states, which are common in photoinduced cycloaddition/cycloreversion reactions, or exclusively intramolecular bond changes, which characterizes most photochromic units. In response to these challenges, we present here the concept of "proximal photocleavage," which combines photochemical crosslinking with a photocleavable linker, enabling a one-time bond formation/cleavage sequence. We report proximal photocleavage methacrylate monomers comprising, in series along the pendant of the methacrylate, a coumarin unit for crosslinking and either a phenacyl or ortho-nitrobenzyl photocleavable group for decrosslinking. We describe the photophysical properties of these monomers and their statistical copolymers with methyl methacrylate, and demonstrate wavelength selective crosslinking and de-crosslinking of thin polymer films.

1. Introduction

Of the many stimuli that chemists use to control materials, light has several unique and advantageous features. Light travels rapidly and can pass through optically transparent barriers in ways that thermal and chemical stimuli cannot.[1] Light can be controlled in space using photomasks and shutter mechanisms to block light,[2–5] lasers to concentrate and direct light,[6–8] and by diffraction/interference interactions to generate precise patterns.[9,10] In addition to these methods of spatiotemporal control, filters and monochromators can be used

to control photon energy to target specific electronic transitions, permitting targeting of different chromophores within a single sample, provided they have some wavelength selectivity.[11–13]

While functionally irreversible reactions are common in functional materials, reversible reactions have distinct advantages in materials applications through additional function and longevity, such as those responsible for rechargeable batteries,[14,15] self-healing materials,[16,17] and biomedical applications.[18,19] Reversible photochemical reactions are a particularly important subclass because they involve high energy excited states that can drive equilibrium away from thermodynamic products. Reversible organic photochemical systems fall roughly into two categories: i) photochromes that undergo an intramolecular change in structure upon irradiation (such as spiropyran, diarylethenes, or azobenzenes), and ii) moieties that perform photochemically allowed cycloadditions that revert upon irradiation with higher energy photons (such as coumarin and anthracene).

Photochromes, such as spiropyran[20] and azobenzene,[21] are stable and efficient for many cycles[22] but have only intramolecular bond forming capabilities. Researchers are pushing the limits on macroscopic changes of photochromes by controlling nanoparticle permeability,[23,24] constructing micelles,[25] expanding hydrogels,[26,27] and preparing both self-healing[28] and self-cleaning[29] polymers. Because of the intramolecular bonding limitation of photochromes, these applications rely on designs such as tuning hydrophobicity[30] and inducing phototaxis.[31] Intermolecular reactivity is generally beyond the scope of photochromic moieties. Photochemical cycloadditions, on the other hand, have intermolecular bonding ability which permits other applications such as photopolymerization[32–34] and polymer crosslinking,[35,36] but they can suffer from significantly less reversibility. Cycloreversion typically requires high energy UV light which can cause photobleaching,[37] and yields photostationary states, which prohibit full recovery of the non-cyclized reactants.[38,39] Researchers have compensated for these inefficiencies of

the cycloreversion reaction by designing materials that function at lower conversion rates,[40,41] or that tolerate very long/intense sessions of high energy irradiation.[42,43]

In considering these two designs, we posit that there are applications of photoresponsive polymers that require only one reversion reaction to function, such as burst release of cargo,[44] multistage polymer networks,[45] and programmed photodegradability.[41] Therefore, a once-reversible photochemical system, where one wavelength of light forms intermolecular bonds, and a second wavelength breaks bonds, could find use. We hypothesize that a design that comprises a photodimer-forming moiety in series with a photocleavable group could combine intermolecular reactivity with more efficient bond breaking. This moiety of two photoreactive groups in sequence allows for photodimerization followed by a 'proximal photocleavage' that could be more efficient than dimer cycloreversion. Although this system is irreversible on the chemical level, on a macroscopic scale it approximates the first cycle of crosslinking and decrosslinking in a photodimer.

2. Results and Discussion

2.1 Design and Synthesis

Our design combines photocrosslinking and photocleavable groups that are physically separated but within the same molecule. We place the crosslinking group at the terminus of a methacrylate monomer pendant, and a proximal photocleavable group between the polymerizable alkene and the crosslinker. Therefore, our overall design **(Figure 1)** intends to enable the bonding and cleavage steps to occur within the same molecule and along the same chain of atoms, but renders different chemical functional groups responsible for these two steps. A similar design involving a combination of light and thiol-ene chemistry has been used in hydrogels,[46] but to our knowledge this is the first time the approach has been done with light as the exclusive stimulus. We chose coumarin as a photocrosslinker in these designs as it is commonly used in polymer applications such as adhesives, lithography, and hydrogel

formation.[40–42,47,48] Although coumarin photo-crosslinks efficiently, the photocleavage reaction is less efficient, requires harsh irradiation conditions, and establishes a photostationary state between cycloaddition and reversion.[40–42] Therefore we designed two monomers that each contain a proximal photocleavable group—either phenacyl ester or *o*-nitrobenzyl ester—both of which have been used for photoinduced de-crosslinking of polymers.[1,49–52] These two photocleavable groups present different electronic and structural properties that can impact their function. For example, while *o*-nitrobenzyl groups are perhaps the most popular class of photocleavable groups in polymer research, their absorbance spectra overlap considerably with that of coumarin between 300-400 nm. Meanwhile, the UV/vis absorbance spectra show noticeable absorbance for the phenacyl groups absorb only below 300 nm, suggesting the possibility for wavelength selectivity with coumarin and phenacyl. In addition, nitroarenes are strong electron acceptors and can therefore quench excited states through photoinduced electron transfer and inhibit radical polymerization reactions.

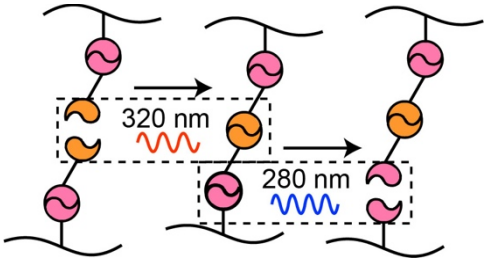

Figure 1. Schematic representation of proximal photocleavage, where photocrosslinking groups and photocleavable groups are bound in series and activated by different wavelengths.

As shown in **Figure 2**, we prepared coumarin-phenacyl monomer **4** using a series of relatively straightforward reactions. Alkylation of 7-hydroxycoumarin with an excess of 1,4-dibromobutane under basic conditions yielded bromoalkylated coumarin **1**. This electrophile serves as the alkylating agent for known phenol **2** to yield diether **3**, using potassium carbonate as the base to minimize any alkylation of the aliphatic alcohol, which we do not

observe as a byproduct. The major side product in this reaction appears to result from elimination of the primary bromide. In addition, we also observed an aldehyde byproduct, consistent with tautomerization of the α-hydroxyketone. Finally, acylation of **3** with methacryloyl chloride yields the monomer **4**, which contains the photocleavable phenacyl and crosslinkable coumarin in series. A similar strategy for synthesis gave coumarin/*o*-nitrobenzyl monomer **7**. Williamson ether synthesis between **1** and the commercially available 5-hydroxy-2-nitrobenzaldehyde yielded diether **5**. We chose DMF as the preferred solvent over acetone or methyl ethyl ketone to avoid aldol chemistry of the aldehyde. Borohydride reduction of the aldehyde in **5** gave primary alcohol **6**, followed again by acylation with methacryloyl chloride to provide the monomer **7**.

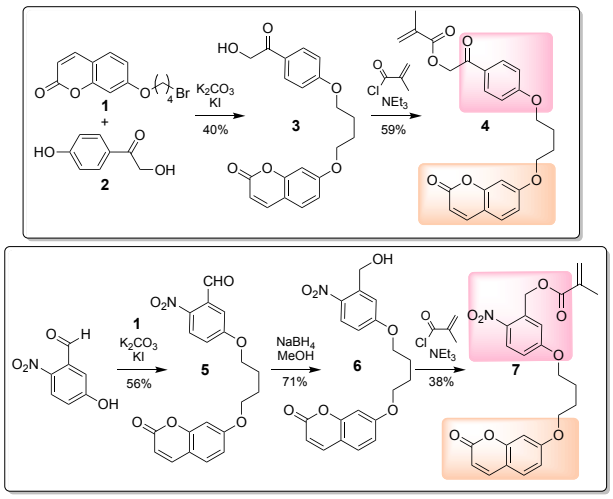

Figure 2. Synthesis for proximal photocleavage monomers **4** and **7**.

We prepared all polymers in this study by free-radical polymerization, initiated by azobisisobutyronitrile (AIBN), forming statistical copolymers of our proximal photocleaving methacrylates **4** and **7** and methyl methacrylate (MMA) as a photochemically inert comonomer. Our polymerization reactions contained feed percentages of **4** or **7** of up to 15% by mole. We were able to determine the incorporation of monomers **4** or **7** into the isolated polymeric products quantitatively using ^{1}H NMR spectroscopy, comparing integrals of a doublet at δ7.65 from the hydrogen on carbon 4 of the coumarin and the singlet at δ3.60 from

the methyl group in MMA. Over the course of this investigation, we prepared four polymers whose properties are summarized **Table 1**. For these four polymers, we use a nomenclature **PX-Y,** in which "**X**" is the identity of the photoreactive monomer used (phenacyl-containing **4** or nitrobenzyl-containing **7**) and "**Y**" is the mole-percent of the photoreactive monomer determined by ^{1}H NMR spectroscopy (2% for a low reactive monomer incorporation; 11 or 14 for higher reactive monomer incorporation). In general, polymers we prepared had number average molecular weights between 10,000 and 50,000 g/mol as determined by gel permeation chromatography using polystyrene standards.

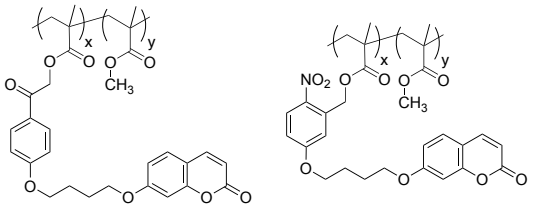

P4-2 x = 0.02, y = 0.98
P4-14 x = 0.14, y = 0.86

P7-2 x = 0.02, y = 0.98
P7-11 x = 0.11, y = 0.89

Chart 1. Structures of the four polymers discussed in this work.

Table 1. Properties of four statistical copolymers comprised of methyl methacrylate and proximal photocleavable monomer.

Polymer	Photocleavable Chromophore	Integration of chromophore [mol%]	Yield [%]	Mn [kD]	PDI
P4-2	Phenacyl	2	71	27	1.4
P4-14	Phenacyl	14	62	14	3.4
P7-2	o-Nitrobenzyl	2	79	13	1.9
P7-11	o-Nitrobenzyl	11	46	44	4.5

2.2 Optical Properties

As these monomers and polymers combine two chromophores in close proximity, we sought to understand the extent to which they interact with each other electronically. We therefore characterized the electronic absorbance spectra of our monomers and polymers and

compared them to those of the independent photocrosslinker and photocleavable groups. As shown in **Figure 3**, the absorbance spectra of monomers **4** and **7** closely resemble linear combinations of the two independent chromophores, with maxima of the three chromophores at 320 nm (coumarin), 314 nm (ortho-nitrobenzyl ester), and 280 nm (phenacyl). These results suggests that no substantial ground state interactions between the chromophores occur in the monomers. UV vis spectra of polymers **P4-14 and P7-1** show the expected features from the contributing chromophores.

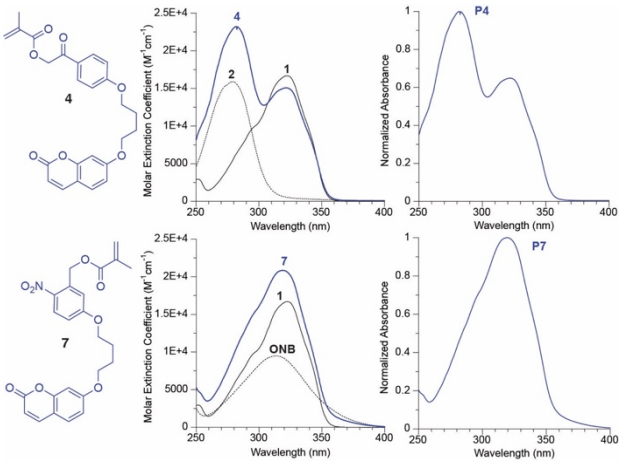

Figure 3. *Left:* UV-vis spectra of monomers **4** and **7** overlayed with spectra of their contributing chromophores. "ONB" is 3-hydroxymethyl-4-nitrophenol. *Right:* UV/vis spectra of corresponding polymers **P4** and **P7**.

Figure 3 reveals that good selectivity for irradiating the coumarin is possible in **P4** monomers, as the phenacyl group at this range of concentrations shows no discernable absorbance at wavelengths greater than approximately 310 nm. Therefore, wavelengths between 310 nm and 365 nm are available for coumarin photodimerization without being absorbed substantially by the phenacyl group. However, the absorbance of the o-nitrobenzyl photocleavable group spans that same region as the coumarin, and extends beyond the coumarin at low energies, to approximately 400 nm, precluding selective irradiation and crosslinking of coumarin in P7 monomers (we note that while it is beyond the scope of this study, selective irradiation of the nitrobenzyl in the presence of this coumarin derivative may be possible).

In addition to determining whether selective absorbance is possible, different chromophores in close proximity offer possibilities of excited state processes such as electron or energy transfer, which could provide additional relaxation pathways for excited states. We therefore measured fluorescence properties of all compounds containing the fluorescent coumarin moiety. As shown in **Figure 4**, monomer **4** has a nearly identical fluorescence spectra and quantum yield as alkylated coumarin **1**, suggesting that the phenacyl excited state of the coumarin does not quench the coumarin excited state. However, the coumarin in monomer **7** has a ~10-fold smaller quantum yield of fluorescence than **1** after accounting for the competing absorption of coumarin and o-nitrobenzyl chromophores. Based on the favorable reduction potential of nitroarenes, we ascribe this quenching to photoinduced electron transfer, which we estimate to have a modest driving force of 0.06 eV based on published electrochemical redox couples and an estimated excited state energy of 3.10 eV.[53–56] A summary of absorbance and fluorescence properties for both single molecules and polymers is given in Table 2.

Table 2. Table of experimental absorbance maxima, extinction coefficients, and fluorescent quantum yields for all compounds in Figure 2 measured in dichloromethane unless otherwise specified. Anthracene in ethanol was used as the standard for relative fluorescence quantum yield measurements.[57] The quantum yields of **7** and **P7-11** are weighted to account for competing absorption from the o-nitrophenol at the excitation wavelength of 320nm.

Compound	λ_{max} (nm)	ε [$10^3 M^{-1} cm^{-1}$]	Coumarin Φ_f [%]
1	320	16.6	1.3
2[a]	280	15.9	N/A
4	280/320	21.5/15.1	1.5
3-HMN[b]	314	9.5	N/A
7	320	20.8	0.2
P4-14	280/320	23.2/20.8	1.5
P7-11	320	17.2	0.3

[a] Compound 2 measured in methanol, for solubility.

[b] 3-HMN is 3-hydroxymethyl-4-nitrophenol, a small molecule analogue for the o-nitrobenzyl chromophore.

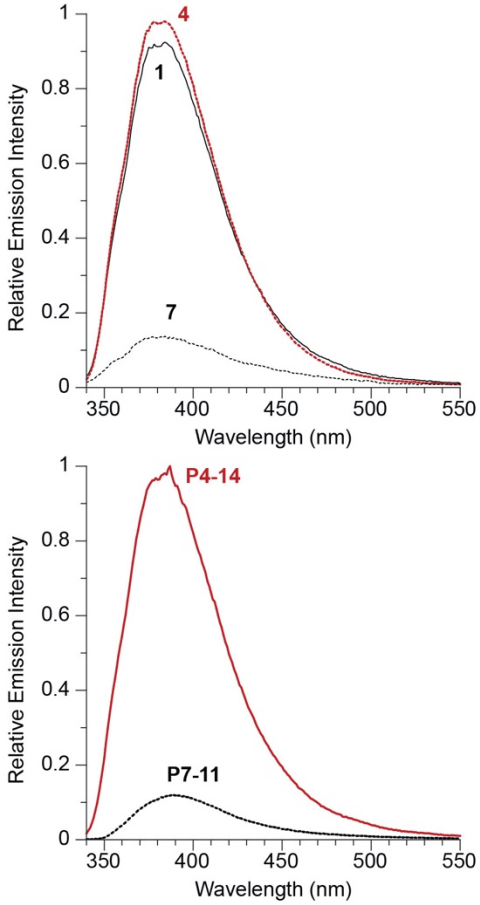

Figure 4. Fluorescence spectra of compounds **1**, **4**, and **7**, showing the fluorescence quenching effect of the o-nitrobenzyl ester (*top*). This quenching effect is also present in polymers **P4** and **P7** (*bottom*).

2.3 Photochemical Reactivity

To demonstrate the impact of sequential crosslinking and cleaving reactions, we integrated the proximal photocleavers into linear methacrylate polymers as reactive side chains and perform the photochemical reactions on these polymers as spun-cast thin films. We evaluated reaction progress and solubility by UV/vis spectrophotometry of the polymer films. The polymers we prepared in this study are initially soluble in organic solvents such as chloroform, toluene, and THF. However, crosslinking reduces the solubility of these films substantially.

Given the optical properties of the two classes of polymers, described above, we focused on phenacyl-containing **P4** polymers to demonstrate sequential reactivity. First, we demonstrated that irradiation of these films at $\lambda > 320$ nm crosslinked the films through

selective coumarin photodimerization (**Figure 5**) Using a 200 W Hg/Xe lamp equipped with a 320 nm longpass filter operating at 81 mW/cm^2, the coumarin absorbance peak at 320 nm decreases in absorbance by approximately 50% over the span of 30 minutes. Meanwhile, the magnitude of the absorbance peak at 280 nm decreases by approximately 10%, which we can attribute to proportional loss of absorbance by coumarin in that region based on the ratio of extinction coefficients of coumarin at 320 and 280 nm.

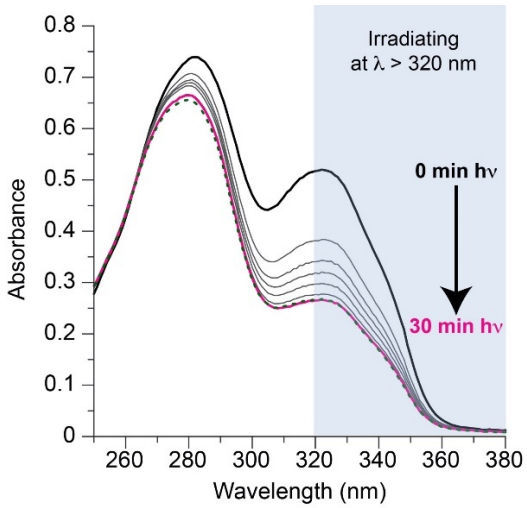

Figure 5. Absorbance spectra of **P4-14** after irradiation with 81mW/cm^2 of λ > 320 nm light at 5-minute intervals, showing the selective activation of the coumarin moiety. Decrease in the peak at 280 nm is consistent with reaction only of the coumarin moiety, as it has some absorbance at 280 nm. The dotted line shows the absorbance spectrum of the film after a soak in chloroform for one hour, demonstrating near total solvent resistance.

Upon reaction of the coumarin as measured by UV/vis, these polymer films become insoluble. We determined solubility by measuring the UV/vis absorbance spectra of films at three stages: i) before irradiation at 320 nm, ii) after irradiation at l > 320 nm, and iii) after soaking for one hour in chloroform. As shown in Figure 6, varying the percent integration of the zip tie monomer affects the efficiency of the crosslinking by coumarin dimerization. Films of polymer P4-14 was completely soluble in chloroform before any irradiation but became completely insoluble after 30 minutes of irradiation at l > 320 nm. Under the same conditions, P7-11 showed 40% loss upon rinsing in chloroform after irradiation. In contrast, P4-02 and P7-02 remained completely soluble after identical irradiation conditions for 30 minutes,

instead requiring approximately 8 hours of irradiation under the same conditions to show any measurable photoinduced insolubility.

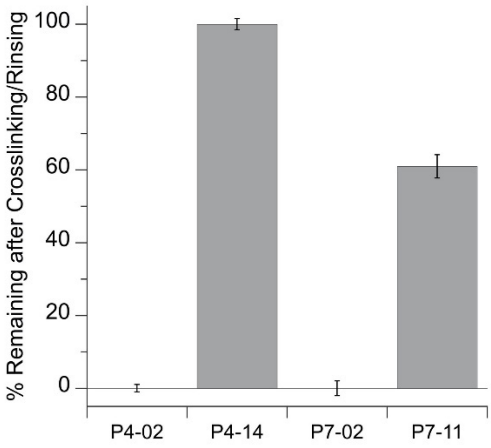

Figure 6. Percentage of films that was rendered insoluble upon irradiating with 30 minutes of $\lambda > 320$ nm light as measured by UV/vis spectrophotometry. Error bars represent standard errors of the mean of five trials.

To demonstrate decrosslinking, we chose polymer **P4-14**, as it crosslinks efficiently because of the coumarin-phenacyl wavelength selectivity, the high percentage integration of the proximal photocleavage monomer, and the higher molecular weight of the polymer sample. We characterize each step of the polymer irradiation process by UV-vis measurements starting with the initial film. After establishing the initial absorbance, we irradiate the film with $\lambda > 320$ nm light to induce crosslinking of the polymer chains through the coumarin units, as described above. At this stage the film is insoluble when submerged in chloroform, whereas the initial film was fully soluble under the same conditions. Subsequent irradiation of the films at $\lambda > 280$ nm can induce photocleavage at the phenacyl units. The resulting films are more soluble than the fully crosslinked ones, although they do not fully dissolve to the extent that the initial film does. **Figure 7** shows an example of the four absorbance spectra obtained from this type of experiment and a graph of the results from five separate trials. By integrating the region where the chromophores absorb for each spectrum, we can calculate film loss relative to the controls for both sets of irradiation conditions. Based

on these data, we estimate that 70-90% of the films of **P4-14** regains solubility in chloroform upon deep UV irradiation.

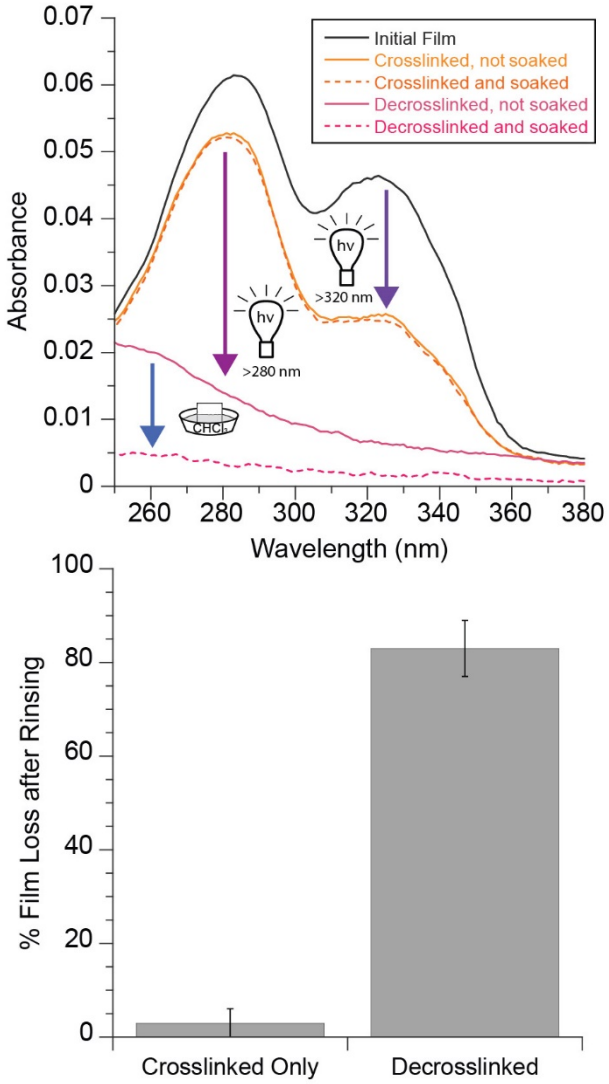

Figure 7 *Top:* Example absorbance spectra of **P4-14** throughout the crosslinking and decrosslinking process. The black trace is the initial film, the solid traces are for a film after crosslinking with λ > 320 nm light (orange), and a film after decrosslinking with λ > 280 nm light (pink). The decrease in the peak at 280 nm is consistent with reaction only of the coumarin moiety, as it has some absorbance at 280 nm. The dashed traces show the the effect of a one hour soak in chloroform on crosslinked (orange) and decrosslinked (pink) films. *Bottom:* Average loss in **P4-14** film absorbance due to chloroform solvation in the region of 250-375nm across 5 trials each of 'crosslinked only' and decrosslinked films.

3. Conclusion

In this study we demonstrate control over the properties of polymer properties through selective photocrosslinking and photocleaving reactions with different chromophores in sequence on a single monomeric unit. Our design includes the straightforward synthetic

pathway for two of these ‘proximal photocleavage’ monomers that are readily integrated into methacrylate polymers. The crosslinking and cleaving chromophores have independent photochemical behavior despite their proximity, except for fluorescence quenching in nitrobenzyl containing compounds. The photocrosslinking can be activated selectively in the presence of a phenacyl photocleavable group to form an insoluble film, while subsequent irradiation targeting the phenacyl group decrosslinks and enables near complete dissolution of polymer films. While this proof-of-concept study has demonstrated promise of this approach, it does have several disadvantages: i) it uses only ultraviolet light, which recent results from the group of Barner-Kowollik may ameliorate due to the increasingly recognized characteristic of photoreactive units to respond best to red-shifted wavelengths beyond their typically recorded absorbance spectra;[58,59] ii) it requires extended irradiation times to induce sufficient photocleavage of the photocleavable groups to re-solubilize the polymer film, which we attribute to the high sensitivity of polymer solubility to low degrees of crosslinking. As a result, this approach is currently not competitive with simpler and more efficient photopolymer systems. Nevertheless, we anticipate that this novel approach of combining different photoreactivie moeites in the same molecule to enable pathway dependent wavelength-orthogonal photoreactions to has the potential to mimic the function of reversible chemistry once, possibly accessing more red-shifted wavelengths, which has potential for applications such as burst release.

4. Experimental Section

Materials

All reactions were performed in dry glassware under an argon atmosphere unless otherwise specified. Silica gel (230-400 mesh) was used for all flash chromatography. Commercially available chemicals were used without purification unless otherwise specified.

Equipment

NMR spectra were acquired using a Bruker Avance III 500 spectrometer. Polymer molecular weights and polydispersity indices (PDI) were determined using a Shimadzu Gel Permeation Chromatograph (GPC) with a UV detector against polystyrene standards. All GPC samples were prepared in tetrahydrofuran (THF) and run with a flow rate of 0.75 mL/min. Absorbance measurements were performed on a Varian Cary 100 spectrophotometer in double beam mode or an Agilent Cary 3500 spectrophotometer in double beam mode. Fluorescence emission spectra were collected on a Quantum Master 4 with a 75 W Xe lamp and a time-correlated single photon counting module. Irradiations were performed with a Newport 200 W Hg/Xe lamp equipped with a condensing lens and a recirculating water filter. Specific irradiation wavelengths were selected using 280 nm and 320 nm longpass filters (Newport), and power density was measured with filters in place. Infrared spectroscopy of films scraped off quartz substrates were performed using a Thermo Scientific Nicolet iS5 FT-IR Spectrometer equipped with an iD1 ATR accessory and a ZnSe crystal. Absorbance and fluorescence measurements of liquid samples were performed in quartz glass cuvettes with 1 cm path lengths and in spectroscopic grade dichloromethane unless otherwise specified. Solid samples for absorbance and irradiation experiments were prepared by spin-casting 2.0 mg/mL solutions (0.5 mL) of polymer in chloroform on 1 in^2, 1 mm thick quartz plate substrates at 50 rpm for 90 seconds, followed by 300 rpm for 30 seconds.

Small Molecule Synthesis

1: Compound **1** was synthesized according to a modified version of a previous procedure.[60] ^{1}H NMR ($CDCl_3$, 500 MHz) δ 7.64 (d, J = 9.5 Hz, 1H; Ar H), 7.37 (d, J = 8.6 Hz, 1H; Ar H), 6.83 (dd, J = 8.6 & 2.3, 1H, Ar H), 6.80 (d, J = 2.1 Hz, 1H; Ar H), 6.25 (d, J = 9.5 Hz, 1H; Ar H), 4.06 (t, J = 6.0 Hz, 2H; CH_2), 3.50 (t, J = 6.5 Hz, 2H, CH_2), 2.09 (quin, J = 6.9 Hz, 2H;

CH_2), 1.99 (quin, 6.6 Hz, 2H; CH_2). ^{13}C NMR ($CDCl_3$, 125 MHz) δ 162.1, 161.2, 155.9, 143.4, 128.8, 113.1, 112.9, 112.6, 101.4, 67.5, 33.2, 29.3, 27.7. λ_{max} (ε) = 320 (16600)

2: Compound **2** was synthesized following previous synthetic procedures without protection of the phenolic OH group.[61] ^1H NMR (CD_3OD, 500 MHz) δ 7.85 (d, J = 8.8 Hz, 2H; Ar H), 6.85 (d, J = 8.8 Hz, 2H; Ar H), 4.81 (s, 2H, CH_2). ^{13}C NMR (MeOD, 125 MHz) δ 198.6, 170.3, 164.3, 131.3, 127.3, 116.5, 65.8. λ_{max} (ε) = 280 (15900)

3: Compounds **1** (0.82 g, 2.8 mmol), **2** (0.40 g, 2.61 mmol), anhydrous potassium carbonate (1.53 g, 11.1 mmol), and potassium iodide (0.11 g, 0.66 mmol) were added to a 100 mL round bottom flask with a magnetic stir bar and 25 mL of methyl ethyl ketone. The mixture was refluxed in an 85 °C oil bath while stirring for 3 hours. The crude mixture was concentrated *in vacuo*, redissolved in dichloromethane, and washed with three aqueous solutions: weakly acidic, weakly basic, and brine. The organic layer was dried with magnesium sulfate and concentrated *in vacuo* to a yellow oil. The oil was purified by flash chromatography with an eluent of 3:1 ethyl acetate/hexanes to afford compound **3** as a colorless solid (0.29 g, 31% yield).

^1H NMR ($CDCl_3$, 500 MHz) δ 7.89 (d, J = 8.9 Hz, 2H; Ar H), 7.64 (d, J = 9.5 Hz, 1H; Ar H), 7.37 (d, J = 8.5 Hz, 1H; Ar H), 6.96 (d, J = 8.5 Hz, 2H; Ar H), 6.83 (dd, J = 8.5 & 2.3 Hz, 1H; Ar H), 6.80 (d, J = 2.0 Hz, 2H; Ar H), 6.26 (d, J = 9.5 Hz, 1H; Ar H), 4.82 (s, 2H, CH_2), 4.12 (m, 4H), 2.04 (m, 4H). ^{13}C NMR ($CDCl_3$, 125 MHz) δ 196.7, 163.7, 162.1, 161.2, 155.9, 143.5, 130.0, 128.8, 114.6, 113.1, 112.9, 112.6, 101.3, 68.0, 67.8, 65.0, 25.8, 25.7. HRMS (ESI) *m*/*z*: $[M + H]^+$ calcd for $C_{21}H_{21}O_6$, 369.1338; found, 369.1335.

4: Compound **3** (0.30 g, 0.81 mmol) in 10 mL of dichloromethane was added to a 50 mL round bottom flask with freshly distilled methacryloyl chloride (1.39 g, 13.3 mmol). The flask

was capped with a rubber septum and vented with an 18-gauge needle, then stirred at 0 °C. Triethylamine (1.45 g, 14.3 mmol) was added dropwise, and the reaction was stirred at room temperature for 16 hours. The crude mixture was concentrated *in vacuo*, redissolved in dichloromethane, and washed with three aqueous solutions: weakly acidic, weakly basic, and brine. The organic layer was dried with magnesium sulfate and concentrated *in vacuo* to a yellow oil. The oil was purified by flash chromatography with an eluent of 1:1 ethyl acetate/hexanes to afford compound **4** as a colorless solid (0.21 g, 59% yield).
^{1}H NMR ($CDCl_3$, 500 MHz) δ 7.91 (d, J = 8.9 Hz, 2H; ArH), 7.64 (d, J = 9.5 Hz, 1H; ArH), 7.37 (d, J = 8.3 Hz, 1H; ArH), 6.95 (d, J = 8.9 Hz, 2H; ArH) 6.84-6.82 (m, 2H), 6.27 (s, 1H), 6.26 (d, J = 9.5 Hz, 1H; ArH), 5.67 (s, 1H), 5.37 (s, 2H, CH_2), 4.11 (m, 4H), 2.02 (m, 7H). ^{13}C NMR ($CDCl_3$, 125 MHz) δ 190.7, 166.9, 163.4, 162.1, 161.2, 155.9, 143.4, 135.6, 130.1, 128.8, 127.4, 126.7, 114.5, 113.1, 112.9, 112.6, 101.4, 68.0, 67.7, 66.0, 25.8, 25.7, 18.3. λ_{max} (ε) = 280 (21500), 320 (15100); HRMS (ESI) *m*/*z*: $[M + H]^+$ calcd for $C_{25}H_{25}O_7$, 437.1600; found, 437.1595.

5: Compound **1** (2.00 g, 6.80 mmol), 5-hydroxy-2-nitrobenzaldehyde (1.76 g, 10.5 mmol), anhydrous potassium carbonate (4.89 g, 35.3 mmol), potassium iodide (0.31 g, 1.86 mmol) were added to a 100 mL round bottom flask with a magnetic stir bar and 25 mL of dry dimethylformamide. The mixture was refluxed for 1 hour with stirring. The mixture was heated in an 85 °C oil bath while stirring for 3 hours. The crude mixture was concentrated *in vacuo*, redissolved in dichloromethane, and washed with deionized water, and then brine. The organic layer was dried with magnesium sulfate and concentrated *in vacuo* to afford compound **5** as a colorless solid (1.46 g, 55.8% yield).
^{1}H NMR ($CDCl_3$, 500 MHz) δ 10.47 (s, 1H), 8.15 (d, J = 9.0 Hz, 1H; ArH), 7.63 (d, J = 9.5 Hz, 1H; ArH), 7.37 (d, J = 8.5 Hz, 1H; ArH), 7.31 (d, J = 2.8 Hz, 1H; ArH), 7.14, (dd, J = 9.1 & 2.8 Hz, 1H; ArH), 6.83 (dd, J = 8.5 & 2.4 Hz, 1H; ArH), 6.80 (d, J = 1.2 Hz, 1H; ArH),

6.25 (d, J = 9.5 Hz, 1H; ArH), 4.19 (t, J = 5.7 Hz, 2H; CH_2), 4.10 (t, J = 5.8 Hz, 2H; CH_2), 2.05 (m, 4H). ^{13}C NMR ($CDCl_3$, 125 MHz) δ 188.5, 163.4, 162.0, 161.1, 155.9, 143.4, 142.2, 134.4, 128.8, 127.3, 118.9, 113.7, 113.2, 112.9, 112.6, 101.3, 68.8, 67.9, 25.7, 25.6. HRMS (ESI) *m*/*z*: $[M + H]^+$ calcd for $C_{20}H_{18}NO_7$, 384.1083; found, 384.1078.

6: Sodium borohydride (0.10 g, 2.7 mmol) was added to a 25 mL round bottom flask with a stir bar and 10 mL of dry methanol, then lowered into an ice bath with stirring for 15 minutes. Compound **5** (0.30 g, 0.78 mmol) was dissolved in 4 mL of dichloromethane, then added dropwise to the 25 mL flask. The flask was stirred for 16 hours. The crude mixture was acidified with hydrochloric acid, extracted three times with dichloromethane, dried over magnesium sulfate, then concentrated *in vacuo* to afford compound **6** as a colorless solid (0.21g, 71% yield).

^1H NMR ($CDCl_3$, 500 MHz) δ 8.18 (d, J = 9.1 Hz, 1H; Ar H), 7.64 (d, J = 9.5 Hz, 1H; Ar H), 7.37 (d, J = 8.3 Hz, 1H; Ar H), 7.25 (d, J = 2.6 Hz, 1H; Ar H), 6.88 (dd, J = 9.1 & 2.7 Hz, 1H; Ar H), 6.84-6.82 (m, 2H), 6.26 (d, J = 9.5 Hz, 1H; Ar H), 5.00 (s, 2H, CH_2), 4.17 (m, 2H), 4.11 (m, 2H), 2.04 (m, 4H). ^{13}C NMR ($CDCl_3$, 125 MHz) δ 163.5, 162.1, 161.3, 155.9, 143.4, 140.5, 140.3, 128.8, 128.0, 114.7, 113.4, 113.1, 113.0, 112.6, 101.3, 68.2, 67.9, 62.9, 30.9, 25.7, 25.6. HRMS (ESI) *m*/*z*: $[M + H]^+$ calcd for $C_{20}H_{20}NO_7$, 386.1240; found, 386.1235.

7: Compound **6** (0.48 g, 1.2 mmol) in 10 mL of dichloromethane was added to a 50 mL round bottom flask with freshly distilled methacryloyl chloride (0.65 g, 6.2 mmol). The flask was capped with a rubber septum and vented with an 18-gauge needle, then stirred at 0 °C. Triethylamine (0.70 g, 6.9 mmol) was added dropwise, and the reaction was stirred at room temperature for 16 hours. The crude mixture was concentrated *in vacuo*, redissolved in dichloromethane, and washed with three aqueous solutions: weakly acidic, weakly basic, and

brine. The organic layer was dried with magnesium sulfate and concentrated *in vacuo* to a yellow oil. The oil was purified by flash chromatography with an eluent of 3:1 ethyl acetate/hexanes to afford compound **7** as a colorless solid (0.36 g, 65% yield). ^{1}H NMR ($CDCl_3$, 500 MHz) δ 8.19 (d, J = 9.1 Hz, 1H; ArH), 7.64 (d, J = 9.5 Hz, 1H; ArH), 7.36 (d, J = 8.4 Hz, 1H; ArH), 7.03 (s, 1H, ArH), 6.89 (dd, J = 9.1, 2.6 Hz, 1H; ArH), 6.83-6.80 (m, 2H), 6.25 (d, J = 9.5 Hz, 1H; ArH), 6.23 (s, 1H), 5.67 (s, 1H), 5.62 (s, 1H, CH_2), 4.13 (m, 2H), 4.10 (m, 2H), 2.03 (m, 4H), 2.01 (s, 3H, CH_3). ^{13}C NMR ($CDCl_3$, 125 MHz) δ 166.6, 163.2, 162.1, 161.1, 155.9, 143.4, 140.3, 135.9, 135.7, 128.8, 128.1, 126.4, 114.1, 113.0, 112.9, 112.6, 101.3, 68.2, 68.0, 63.4, 25.7, 25.7, 18.4. λ_{max} (ε) = 320 (20800); HRMS (ESI) *m*/*z*: $[M + H]^+$ calcd for $C_{24}H_{24}NO_8$, 454.1502; found, 454.1500.

Polymer Synthesis: **General Procedure:** Compound **4** or **7**, azobisisobutyronitrile, and toluene were added to a 10 mL conical flask with a magnetic stir bar and sparged with argon for 20 minutes. Methyl methacrylate was filtered through neutral alumina and added to the flask. Sparging was continued for an additional 10 minutes, and then the flask was covered with a septum cap and lowered into a 65°C oil bath with stirring at 300 rpm overnight (~16 hours). The crude mixture was concentrated *in vacuo* to remove the toluene, then dissolved in a minimum amount of dichloromethane and precipitated in methanol. Precipitated polymer was collected by a combination of decanting and centrifugation at 4000 rpm for 5 minutes. Polymers were reprecipitated using this procedure up to 5 times. The purified polymer was redissolved in dichloromethane, and transferred to a scintillation vial for storage. After drying, all polymers are transparent and colorless.

P4-02:

Compound **4** (0.09 g, 0.3 mmol), azobisisobutyronitrile (AIBN) (0.05 g, 0.3 mmol), methyl methacrylate (1.16 g, 11.5mmol), (0.89 g, 71% yield, M_n: 27 kDa; M_w: 38 kDa). ^{1}H NMR

($CDCl_3$, 500 MHz) δ 7.93-7.87, 7.67-7.63, 7.40-7.36, 6.98-6.93, 6.29-6.23, 5.24-5.18, 3.68-3.50, 2.12-0.32.

P4-14

Compound **4** (0.22 g, 0.51 mmol), AIBN (0.03 g, 0.2 mmol), methyl methacrylate (0.32 g, 3.2 mmol), (0.34 g, 62% yield, M_n: 14 kDa; M_w: 48 kDa). ^{1}H NMR ($CDCl_3$, 500 MHz) δ 7.94-7.79, 7.67-7.57, 7.40-7.31, 7.02-6.69, 6.28-6.17, 5.33-5.06, 4.20-3.93, 3.80-3.39, 2.26-0.57.

P7-02

Compound **7** (0.02 g, 0.4 mmol), AIBN (0.02 g, 0.2 mmol), methyl methacrylate (0.18 g, 1.8 mmol), (0.16 g, 79% yield, M_n: 13 kDa; M_w: 25 kDa). ^{1}H NMR ($CDCl_3$, 500 MHz) δ 8.25-8.13, 7.70-7.63, 7.44-7.37, 7.21-7.14, 6.99-6.92, 6.88-6.80, 6.30-6.24, 5.51-5.35, 4.26-4.08, 3.71-3.46, 2.19-0.66.

P7-11

Compound **7** (0.08 g, 0.2 mmol), AIBN (0.01 g, 0.07 mmol), methyl methacrylate (0.19 g, 1.9 mmol) (0.12 g, 46% yield, M_n: 44 kDa; M_w: 198 kDa). ^{1}H NMR ($CDCl_3$, 500 MHz) δ 8.25-8.03, 7.73-7.60, 7.43-7.33, 7.19-7.06, 6.98-6.72, 6.29-6.19, 5.50-5.27, 4.25-4.02, 3.69-3.41, 2.19-0.60.

Supporting Information

Supporting Information is available from the Wiley Online Library or from the author.

Acknowledgements

This material is based upon work supported by the National Science Foundation under Grant No. CHE-1806263.

Received: ((will be filled in by the editorial staff))

Revised: ((will be filled in by the editorial staff))

Published online: ((will be filled in by the editorial staff))

References

[1] M. J. Feeney, S. W. Thomas, *Langmuir* **2019**, *35*, 13791.
[2] J. J. Richardson, J. Cui, M. Björnmalm, J. A. Braunger, H. Ejima, F. Caruso, *Chem. Rev.* **2016**, *116*, 14828.
[3] X. Hu, Z. Qureishi, S. W. Thomas, *Chem. Mater.* **2017**, *29*, 2951.
[4] B. Lamontagne, N. R. Fong, I.-H. Song, P. Ma, P. J. Barrios, D. Poitras, *J. MicroNanolithography MEMS MOEMS* **2019**, *18*, 040901.
[5] M. M. Hamedi, V. E. Campbell, P. Rothemund, F. Güder, D. C. Christodouleas, J.-F. Bloch, G. M. Whitesides, *Adv. Funct. Mater.* **2016**, *26*, 2446.
[6] R. Brighenti, M. P. Cosma, L. Marsavina, A. Spagnoli, M. Terzano, *J. Mater. Sci.* **2021**, *56*, 961.
[7] F. Sima, K. Sugioka, R. M. Vázquez, R. Osellame, L. Kelemen, P. Ormos, *Nanophotonics* **2018**, *7*, 613.
[8] Z. Tarle, A. Meniga, M. Ristic, J. Sutalo, G. Pichler, *Eur. J. Oral Sci.* **1995**, *103*, 394.
[9] L. Mulko, H. Heffner, S. Bongiovanni Abel, R. Baumann, D. Martín, F. Schell, A. F. Lasagni, *ACS Appl. Polym. Mater.* **2022**, *4*, 8715.
[10] C. A. Barbero, D. F. Acevedo, *Nanomanufacturing* **2022**, *2*, 229.
[11] V. San Miguel, C. G. Bochet, A. del Campo, *J. Am. Chem. Soc.* **2011**, *133*, 5380.
[12] A. Rodrigues-Correia, X. M. M. Weyel, A. Heckel, *Org. Lett.* **2013**, *15*, 5500.
[13] R. Weinstain, T. Slanina, D. Kand, P. Klán, *Chem. Rev.* **2020**, *120*, 13135.
[14] B. Dunn, H. Kamath, J.-M. Tarascon, *Science* **2011**, *334*, 928.
[15] G. Plante, *The Storage Of Electrical Energy*, Paul Bedford, **1859**.
[16] P. Chakma, D. Konkolewicz, *Angew. Chem. Int. Ed.* **2019**, *58*, 9682.
[17] K. Jud, H. H. Kausch, J. G. Williams, *J. Mater. Sci.* **1981**, *16*, 204.
[18] M. J. Webber, E. A. Appel, E. W. Meijer, R. Langer, *Nat. Mater.* **2016**, *15*, 13.
[19] P. Müller, M. Sahlbach, S. Gasper, G. Mayer, J. Müller, B. Pötzsch, A. Heckel, *Angew. Chem.* **n.d.**, *n/a*, DOI 10.1002/ange.202108468.
[20] R. Klajn, *Chem. Soc. Rev.* **2013**, *43*, 148.
[21] H. M. D. Bandara, S. C. Burdette, *Chem. Soc. Rev.* **2012**, *41*, 1809.
[22] B. Razavi, A. Abdollahi, H. Roghani-Mamaqani, M. Salami-Kalajahi, *Polymer* **2020**, *187*, 122046.
[23] X. Wang, J. Hu, G. Liu, J. Tian, H. Wang, M. Gong, S. Liu, *J. Am. Chem. Soc.* **2015**, *137*, 15262.
[24] H. Zhao, S. Sen, T. Udayabhaskararao, M. Sawczyk, K. Kučanda, D. Manna, P. K. Kundu, J.-W. Lee, P. Král, R. Klajn, *Nat. Nanotechnol.* **2016**, *11*, 82.
[25] S. Son, E. Shin, B.-S. Kim, *Biomacromolecules* **2014**, *15*, 628.
[26] C. Li, A. Iscen, L. C. Palmer, G. C. Schatz, S. I. Stupp, *J. Am. Chem. Soc.* **2020**, *142*, 8447.
[27] C. Li, A. Iscen, H. Sai, K. Sato, N. A. Sather, S. M. Chin, Z. Álvarez, L. C. Palmer, G. C. Schatz, S. I. Stupp, *Nat. Mater.* **2020**, 1.
[28] Z. Zhang, M. Chen, I. Schneider, Y. Liu, S. Liang, S. Sun, K. Koynov, H.-J. Butt, S. Wu, *Macromolecules* **2020**, *53*, 8562.
[29] P. Kaner, X. Hu, S. W. Thomas, A. Asatekin, *ACS Appl. Mater. Interfaces* **2017**, *9*, 13619.

[30] Y. Yan, M. Feeney, L. M. Davis, S. W. I. Thomas, *ACS Appl. Polym. Mater.* **2022**, *4*, 5380.
[31] A. Natansohn, P. Rochon, *Chem. Rev.* **2002**, *102*, 4139.
[32] L. Addadi, M. Lahav, *J. Am. Chem. Soc.* **1978**, *100*, 2838.
[33] M. V. Tsurkan, C. Jungnickel, M. Schlierf, C. Werner, *J. Am. Chem. Soc.* **2017**, *139*, 10184.
[34] S. C. Ligon, R. Liska, J. Stampfl, M. Gurr, R. Mülhaupt, *Chem. Rev.* **2017**, *117*, 10212.
[35] L. M. Minsk, W. P. V. Deusen, E. M. Robertson, *Photosensitization of Polymeric Cinnamic Acid Esters*, **1954**, US2670287A.
[36] Y. Chen, C.-S. Jean, *J. Appl. Polym. Sci.* **1997**, *64*, 1749.
[37] J. Ling, M. Z. Rong, M. Q. Zhang, *Polymer* **2012**, *53*, 2691.
[38] Q. Fu, L. Cheng, Y. Zhang, W. Shi, *Polymer* **2008**, *49*, 4981.
[39] Y. Chen, K.-H. Chen, *J. Polym. Sci. Part Polym. Chem.* **1997**, *35*, 613.
[40] Q. Chen, Q. Yang, P. Gao, B. Chi, J. Nie, Y. He, *Ind. Eng. Chem. Res.* **2019**, *58*, 2970.
[41] C. Zhao, C. Shao, X. Yu, D. Yang, J. Wei, *J. Phys. Chem. C* **2017**, *121*, 11428.
[42] L. Wang, X. Ma, L. Wu, Y. Sha, B. Yu, X. Lan, Y. Luo, Y. Shi, Y. Wang, Z. Luo, *Eur. Polym. J.* **2021**, *144*, 110213.
[43] C. P. Kabb, C. S. O'Bryan, C. C. Deng, T. E. Angelini, B. S. Sumerlin, *ACS Appl. Mater. Interfaces* **2018**, *10*, 16793.
[44] V. Brega, F. Scaletti, X. Zhang, L.-S. Wang, P. Li, Q. Xu, V. M. Rotello, S. W. Thomas, *ACS Appl. Mater. Interfaces* **2019**, *11*, 2814.
[45] D. P. Nair, N. B. Cramer, J. C. Gaipa, M. K. McBride, E. M. Matherly, R. R. McLeod, R. Shandas, C. N. Bowman, *Adv. Funct. Mater.* **2012**, *22*, 1502.
[46] C. A. DeForest, K. S. Anseth, *Nat. Chem.* **2011**, *3*, 925.
[47] B. Razavi, M. Soleymani-Kashkooli, M. Salami-Kalajahi, H. Roghani-Mamaqani, *J. Mol. Liq.* **2021**, *344*, 117766.
[48] T. Defize, J.-M. Thomassin, H. Ottevaere, C. Malherbe, G. Eppe, R. Jellali, M. Alexandre, C. Jérôme, R. Riva, *Macromolecules* **2019**, *52*, 444.
[49] K. Inomata, S. Kawasaki, A. Kameyama, T. Nishikubo, *React. Funct. Polym.* **2000**, *45*, 1.
[50] T. G. Brevé, M. Filius, S. Weerdenburg, S. J. van der Griend, T. P. Groeneveld, A. G. Denkova, R. Eelkema, *Chem. – Eur. J.* **2022**, *28*, e202103523.
[51] S. Bian, J. Zheng, W. Yang, *J. Polym. Sci. Part Polym. Chem.* **2014**, *52*, 1676.
[52] Z. C. Smith, D. M. Meyer, M. G. Simon, C. Staii, D. Shukla, S. W. Thomas, *Macromolecules* **2015**, *48*, 959.
[53] C. A. M. Seidel, A. Schulz, M. H. M. Sauer, *J. Phys. Chem.* **1996**, *100*, 5541.
[54] A. Kuhn, K. G. von Eschwege, J. Conradie, *J. Phys. Org. Chem.* **2012**, *25*, 58.
[55] V. V. Pavlishchuk, A. W. Addison, *Inorganica Chim. Acta* **2000**, *298*, 97.
[56] Y. Jing, B. P. Chaplin, *Environ. Sci. Technol.* **2017**, *51*, 2355.
[57] W. H. Melhuish, *J. Phys. Chem.* **1961**, *65*, 229.
[58] I. M. Irshadeen, S. L. Walden, M. Wegener, V. X. Truong, H. Frisch, J. P. Blinco, C. Barner-Kowollik, *J. Am. Chem. Soc.* **2021**, *143*, 21113.
[59] S. L. Walden, J. A. Carroll, A.-N. Unterreiner, C. Barner-Kowollik, *Adv. Sci.* **2024**, *11*, 2306014.
[60] P. Feng, J. Zhu, Z. Cheng, Z. Zhang, X. Zhu, *Polymer* **2007**, *48*, 5859.
[61] R. S. Givens, K. F. Stensrud, in *Encycl. Reag. Org. Synth.*, American Cancer Society, **2009**.

Proximal Photocleavage: Controlling Polymer Solubility Through Pathway Dependent Wavelength-Orthogonal Photoreactions